COMPUTER MODELING OF PULSED EDDY-CURRENTS IN CONDUCTING MATERIALS FOR NDT PURPOSES

Reinhold Ludwig and Xiao-Wei Dai
Department of Electrical Engineering
Worcester Polytechnic Institute
Worcester, Massachusetts 01609

Ramisamy Palanisamy
Timken Research
The Timken Company
Canton, Ohio 44706

INTRODUCTION

The numerical modeling of single frequency eddy-current phenomena based on the magnetic vector potential has been successfully applied to many NDT applications [1-3]. Despite the considerable wealth of sinusoidal eddy-current literature, the numerical modeling of pulsed eddy-currents has received little attention. Most of the recent finite element transient eddy-current NDT modeling [4,5] employs a variational time-domain formulation for 2D and axisymmetric geometries. Since this model was tested against experimental measurements, it lacks rigorous quantitative verification required to be a useful NDT design tool.

The purpose of this paper is two-fold. In the first part a weighted residual finite element formulation for transient magnetic vector potentials and eddy-current field predictions is introduced. In the second part, an analytical theory is presented which allows direct comparison with the numerical formulation, thus enabling much-needed quantitative testing.

PULSED EDDY-CURRENT FINITE ELEMENT FORMULATION

The underlying equation governing pulsed eddy-current phenomena is the inhomogeneous diffusion equation

$$\nabla^2 \mathbf{A} - \mu\sigma \frac{\partial \mathbf{A}}{\partial t} = -\mu \mathbf{J} \tag{1}$$

where μ, σ are total magnetic permeability and electric conductivity. **A** and **J** become for 2D and axisymmetric geometries single component magnetic vector component A and source current density J. Forming an inner product over the solution domain Ω

$$< \left(\nabla^2 A - \mu\sigma \frac{\partial A}{\partial t} + \mu J \right) \phi_i > = 0 \tag{2}$$

Review of Progress in Quantitative Nondestructive Evaluation, Vol. 9
Edited by D.O. Thompson and D.E. Chimenti
Plenum Press, New York, 1990

with the brackets < > denoting volume integration and ϕ_i is a polynomial weighting function over the nodes i in the discretized solution domain Ω. Applying Gauss' law to (2) and assuming a Galerkin-type trial function approach

$$A = \sum_j A_j \phi_j \quad , \quad J = \sum_j J_j \phi_j \tag{3}$$

where A_j, J_j are discrete constant nodal values throughout the domain. After lengthy manipulations, one obtains a set of algebraic equations which can be expressed in matrix notation as

$$[S]\{A\} + [C]\{\dot{A}\} + [D]\{J\} = \{Q\} \tag{4}$$

where the [S], [C], [D] matrices contain the domain integrals involving combinations of the polynomial approximation functions ϕ_i. The nodal point values for the vector potential, its time derivative, and current are given in the column vectors {A}, {Å}, and {J}. {Q} contains the Neumann boundary conditions. Using a backward difference formula to replace the time derivative, permits recasting (4) in a time-stepping algorithm

$$\left([S] + \frac{1}{\Delta t}[C]\right)\{A\}_{t+\Delta t} = \frac{1}{\Delta t}[C]\{A\}_t + \{Q\}_t \tag{5}$$

The required initial condition $\{A\}_0$ is obtained as the static solution to (5) by neglecting the [C] matrix for the first time step. Once the time slices $\{A\}_t$ are determined, the induced eddy-currents $\{J_e\}$ can be computed according to

$$\{J_e\}_t = \frac{\sigma}{\Delta t}(\{A\}_t - \{A\}_{t-\Delta t}) \cdot \tag{6}$$

ANALYTICAL HALF-SPACE FORMULATION

The analytical solution approach involves either an infinitely long wire or a wire loop suspended over a conducting half-space as shown in Fig. 1.

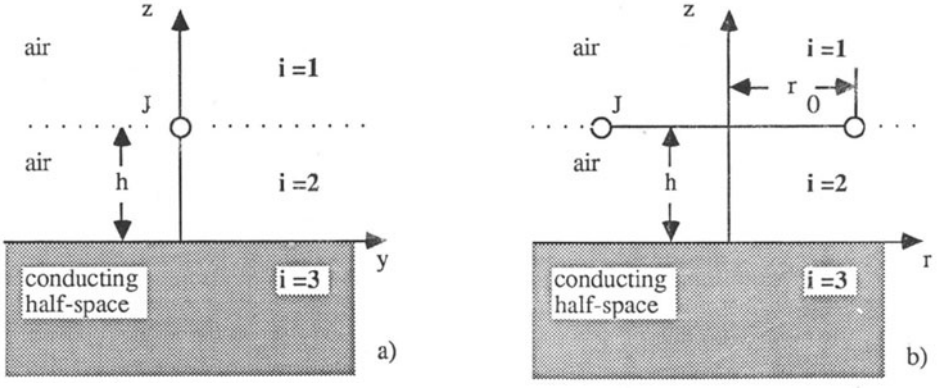

Fig.1. Geometric arrangements for current source suspended over a conducting half-space in a) 2D rectangular coordinate system and b) axisymmetric cylindrical coordinate system.

The sinusoidal vector potential in the three regions in 2D rectangular coordinates can be cast as follows [6]

$$A_1 = \int_0^\infty C_1(k)\ \cos ky\ e^{-k(z-h)}\ dk \tag{7}$$

$$A_2 = \int_0^\infty [C_2(k)\ e^{k(z-h)} + D_2(k)\ e^{-kz}]\ \cos ky\ dk \tag{8}$$

$$A_3 = \int_0^\infty C_3(k)\ \cos ky\ e^{\gamma z}\ dk \tag{9}$$

where $\gamma^2 = k^2 + j\frac{2}{\delta^2}$ and $\delta^2 = \frac{2}{\omega\sigma\mu_0\mu_r}$

The unknown coefficients $C_i(k)$ and $D_2(k)$ are determined by applying appropriate boundary conditions across the interfaces. Following an inverse Laplace-transform technique, it can be shown [7] that the eddy-current density is given by

$$J_e(y,z,t) = \frac{-I_0 u(t)}{\pi}\int_0^\infty e^{-kh}\exp\left(-\frac{k^2 t}{\sigma\mu_0\mu_r}\right)\left[\sqrt{\frac{\sigma\mu_0\mu_r}{\pi t}}\exp\left(\frac{-z^2\sigma\mu_0\mu_r}{4t}\right) + \right.$$

$$\left. - k\exp\left(-zk\mu_r + \frac{k^2\mu_r t}{2\sigma\mu_0}\right)\operatorname{erfc}\left(-\frac{z}{2}\sqrt{\frac{\sigma\mu_0\mu_r}{t}} + \mu_r k\sqrt{\frac{t}{\sigma\mu_0\mu_r}}\right)\right]\cos(ky)\ dk \tag{10}$$

where it is assumed that the excitation current is a step current $I_0u(t)$ and erfc( ) denotes the error function. A similar argument based on an inverse Hankel transform yields for the axisymmetric case

$$J_e(r,z,t) = -I_0 u(t)\ r_0\int_0^\infty \lambda\ J_1(\lambda r_0)\ J_1(\lambda r)\ e^{-\lambda h}\exp\left(\frac{-t\lambda^2}{\sigma\mu_0\mu_r}\right)\times$$

$$\left[\sqrt{\frac{\sigma\mu_0\mu_r}{\pi t}}\exp\left(\frac{-z\,\sigma\mu_0\mu_r}{4t}\right) - \lambda\exp\left(-z\lambda\mu_r + \frac{t\lambda^2\mu_r}{2\sigma\mu_0}\right)\times\right.$$

$$\left.\operatorname{erfc}\left(-\frac{z}{2}\sqrt{\frac{\sigma\mu_0\mu_r}{t}} + \mu_r\lambda\sqrt{\frac{t}{\sigma\mu_0\mu_r}}\right)\right]\ d\lambda \tag{11}$$

with $J_1( )$ being the Bessel function of first order and r_0 the radius of the wire loop.

SIMULATIONS

Fig. 2 compares the 2D numerical eddy-current predictions with the analytical expression (10) in the conducting half-space. As expected, the numerical model has difficulties following the initial sharp current rise at the surface due to the step excitation, but as time increases remarkable agreement is achieved.

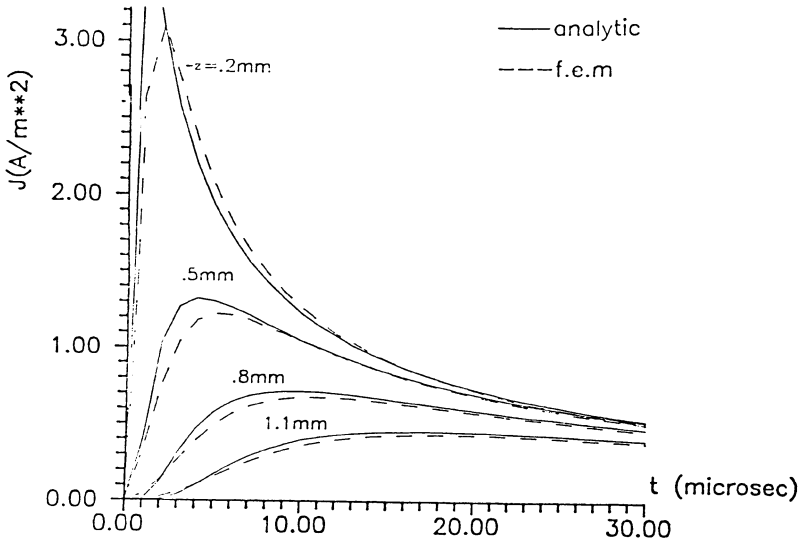

Fig. 2. Comparison of numerical versus analytical temporal eddy-current distribution at y=0 and various depths z into the conducting (σ= $3.5x10^7 Sm^{-1}$) half-space based on an excitation current density of 25 Amp/m^2.

Alternatively, Fig. 3 provides a comparison of the two methods for various instances in time as a function of depth.

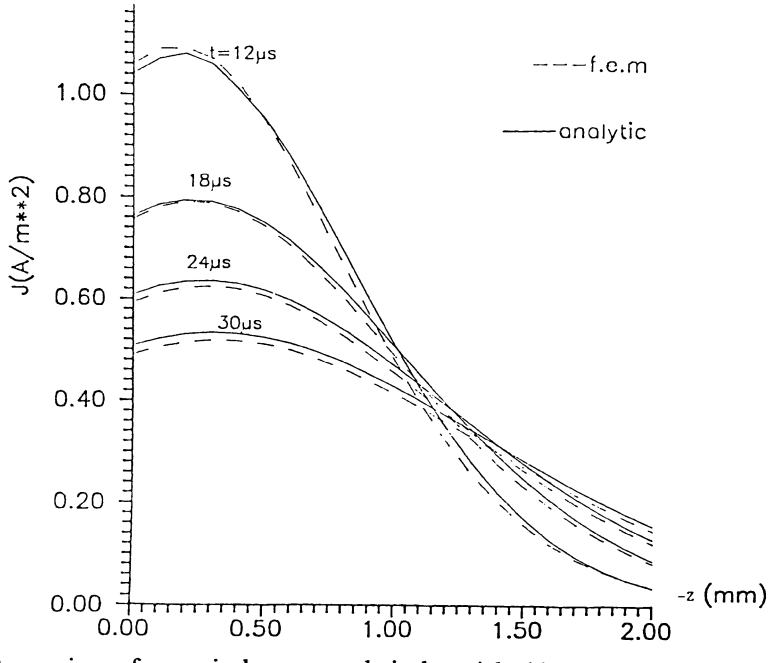

Fig. 3. Comparison of numerical versus analytical spatial eddy-current distribution along the z axis at various time instances in the half-space. The input data are the same as in Fig. 2.

The axisymmetric numerical predictions are compared with the analytical expression (11) for an arbitrarily chosen radius of r=0.9 mm. Again both methods show excellent quantitative agreement as seen in Figures 4 and 5.

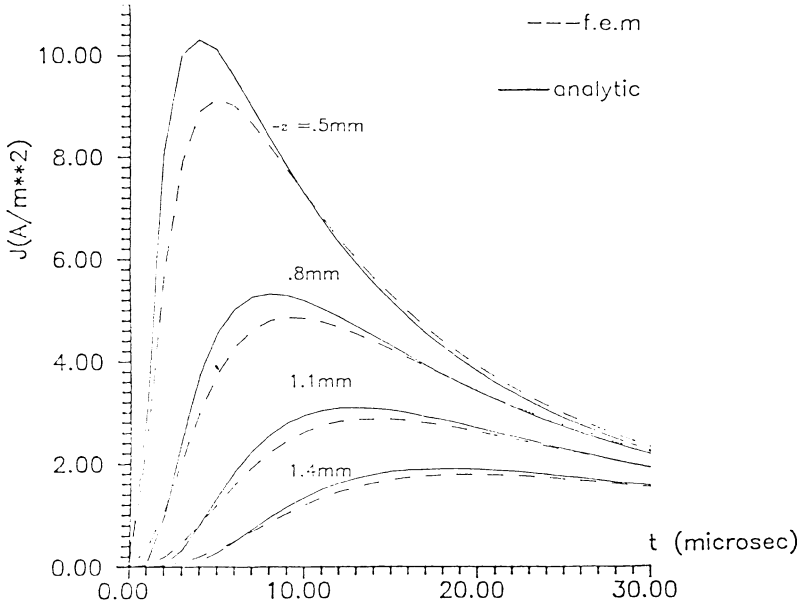

Fig. 4. Comparison of numerical versus analytical temporal eddy-current distribution at various depths z in the cylindrical half-space. The excitation current density is 2500 Amp/m^2.

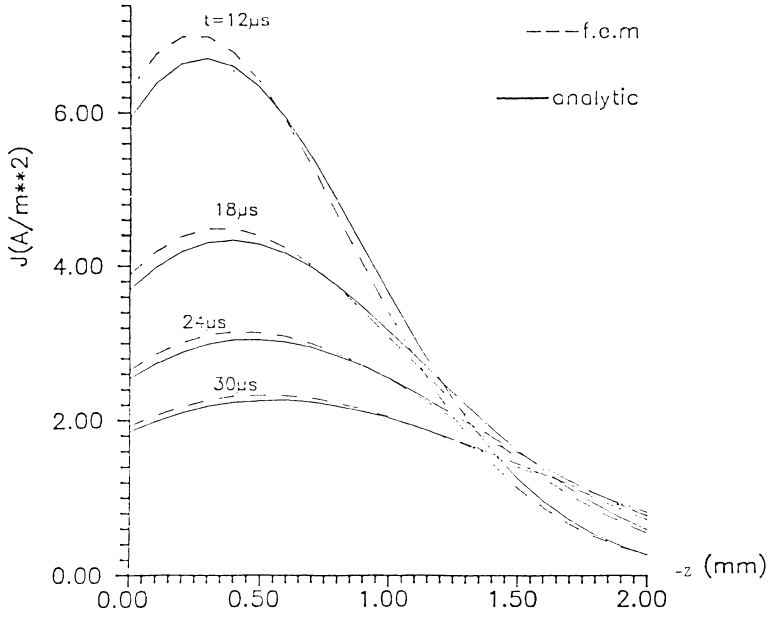

Fig. 5. Comparison of numerical versus analytical spatial eddy-current distribution in the cylindrical half-space.

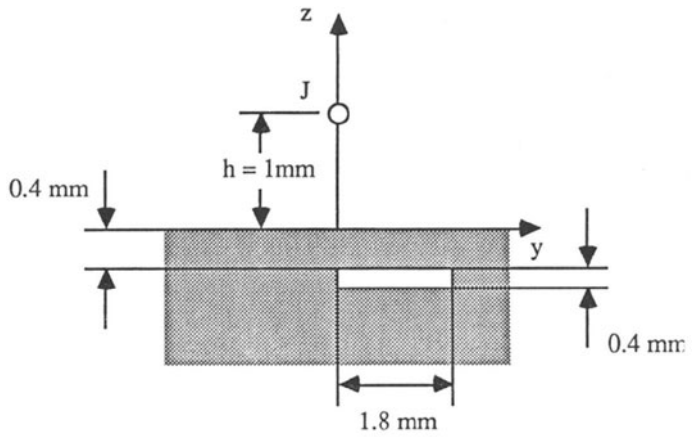

Fig. 6. Geometry of infinite wire (current density 2500 Amp/m^2) suspended over flawed conducting half-space.

In order to demonstrate the power of this numerical approach, the transient field interaction with a sub-surface defect of $\sigma=10^3$ Sm^{-1} is modeled (Fig. 6).

The resulting eddy-current distribution in Fig. 7 is displayed in a combined spatial and temporal distribution. The change in conductivity due to the presence of the flaw is clearly detectable in the discontinuity in the induced eddy-currents.

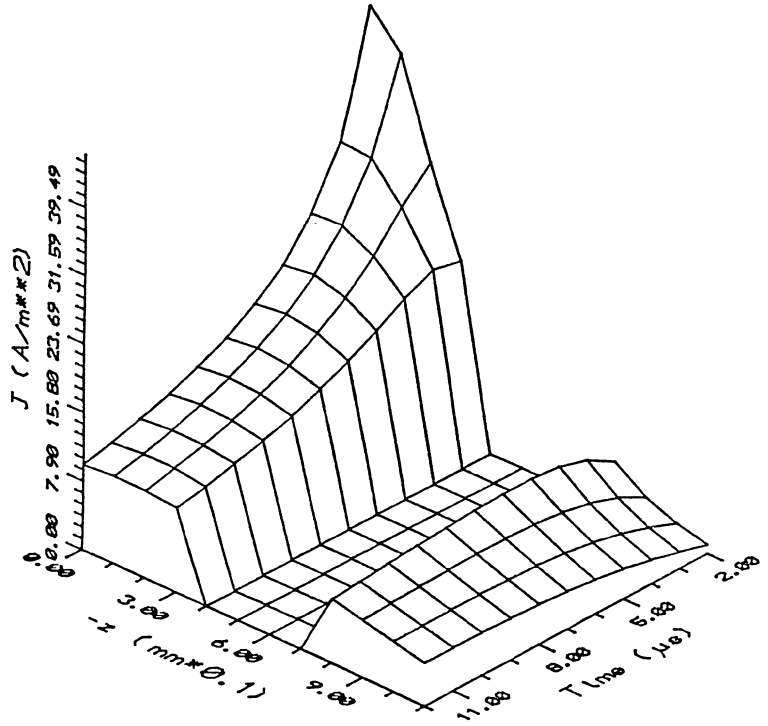

Fig. 7. Combined spatial and temporal eddy-current distribution in the flawed rectangular half-space based on Fig. 6.

CONCLUSIONS

A weighted residual transient finite element formulation has been developed and its correctness is tested against a novel analytical method in the time domain both for the 2D rectangular and axisymmetric case. The numerical simulations required 32,400 linear, triangular elements and typical time steps of 100(=100μs) consume approximately 80 minutes of CPU time on HP 9000 series 350 workstation.

Having confirmed the correctness of the numerical formulation, it now remains to extend the modeling to realistic NDT situations for which, in general, no explicit analytical models are available. Further work also includes nonlinearity due to the hysteresis effect in ferromagnetic materials.

ACKNOWLEDGEMENT

This project has been supported by the Nondestructive Evaluation and Sensor Technology Department of Timken Research, The Timken Company, Canton Ohio.

REFERENCES

1. R. Palanisamy and W. Lord, "Finite Element Modeling of Electromagnetic NDT Phenomena," IEEE Trans. Magn., vol. MAG-16, no. 5, pp. 1083-1085, Sept. 1980.
2. R. Palanisamy, "Finite Element Modeling of Eddy-Current Nondestructive Testing Phenomena," Ph.D. dissertation, Dept. of Electrical Engineering, Colorado State University, 1983.
3. R. Palanisamy and W. Lord, "Interaction of Support Plate and Defect Eddy-Current Trajectories in Steam Generator Tubing NDT," Mat. Evaluation, vol. 39, no. 7, pp. 651-655, June 1981.
4. B. L. Allen, "Finite Element Modeling of Pulsed Electromagnetic NDT Phenomena," M.S. thesis, Dept. of Electrical Engineering, Colorado State University, 1983.
5. B. Allen and W. Lord, "Finite Element Modeling of Pulsed Eddy Current Phenomena," Rev. Progr. Quantitative Nondestructive Evaluation, D. O. Thompson and D. E. Chimenti eds., vol. 3A, pp. 589-597, 1984.
6. D. L. Stoll, The analysis of Eddy-Currents, Clarendon Press, Oxford, England, 1974.
7. R. Ludwig and X.-W. Dai, "Numerical and Analytical Modeling of Pulsed Eddy-Currents in a Conducting Half-Space," to appear in IEEE Trans. Magn.